COMPDYN 2013
4th ECCOMAS Thematic Conference on
Computational Methods in Structural Dynamics and Earthquake Engineering
M. Papadrakakis, V. Papadopoulos, V. Plevris (eds.)
Kos Island, Greece, 12–14 June 2013

SEISMIC RELIABILITY ASSESSMENT OF CLASSICAL COLUMNS SUBJECTED TO NEAR SOURCE GROUND MOTIONS

Ioannis Psycharis[1*], Michalis Fragiadakis[2], Ioannis Stefanou[3]

[1]School of Civil Engineering, National Technical University of Athens, Greece
ipsych@central.ntua.gr,

[2]Department of Civil and Environmental Engineering, University of Cyprus
mfrag@ucy.ac.cy,

[3]Université Paris-Est, Laboratoire Navier (UMR 8205), CNRS, ENPC, IFSTTAR,
F-77455 Marne-la-Vallée
ioannis.stefanou@enpc.fr

Keywords: Classical monuments, multidrum masonry columns, risk assessment, 3D Distinct Element Method (DEM), performance-based design.

Abstract. *A methodology for the performance-based seismic risk assessment of classical columns is presented. Classical columns are articulated structures, made of several discrete bulgy stone blocks (drums) put one on top of the other without mortar. Despite its apparent instability, this structural system is, in general, earthquake resistant, as proven from the fact that many classical monuments have survived many strong earthquakes over the centuries. Nevertheless, due to the fundamental non-linear character and the sensitivity of their response, the quantitative assessment of their reliability and the understanding of their dynamic behaviour are not easy. Consequently, the derivation of general remarks regarding their seismic risk is not trivial. In order to understand the dynamic behaviour and estimate the capacity of multidrum columns, a seismic risk assessment methodology is performed using Monte Carlo simulation with synthetic ground motions. The ground motions adopted contain a high and a low frequency component, combining the stochastic method and a simple analytical pulse model in order to simulate the directivity pulse contained in near source ground motions. Fragility curves are produced first conditional on magnitude and fault distance and then using a scalar intensity measure. The deterministic model for the numerical analysis of the system is three dimensional and is based on the Discrete Element Method (3D DEM). Fragility analysis demonstrates some of the salient features of these spinal systems and provides useful results regarding their reliability and decision-making during restoration process.*

1 INTRODUCTION

Several investigators have examined the seismic response of classical monuments and also that of stacks and of rigid bodies. These studies were analytical, numerical or experimental, mostly using two-dimensional models (e.g. [1] – [6] among others) and lesser using three-dimensional ones (e.g. [7] – [12]). It was shown that the response is non-linear and sensitive even to small changes of the parameters. These characteristics are evident even to the simplest case of a rocking rigid block (Housner [13]).

Previous analyses of the seismic response of classical columns have shown that these structures, despite their apparent instability to horizontal loads, are, in general, earthquake resistant (Psycharis *et al*. [5]), which is also proven from the fact that many classical monuments built in seismic prone areas have survived for almost 2500 years. However, many others have collapsed.

In general, the vulnerability of ancient monuments to earthquakes depends on two main parameters (Psycharis, *et al*. [5]): the size of the structure and the predominant period of the ground motion. Concerning the size, larger columns are more stable than smaller ones with the same aspect ratio of dimensions. Concerning the period of the excitation, it affects significantly the response and the possibility of collapse, with low-frequency earthquakes being much more dangerous than high-frequency ones. In this sense, near field ground motions, which contain long-period directivity pulses, might bring these structures to collapse.

The assessment of the seismic reliability of a monument is a prerequisite for the correct decision making during a restoration process. The seismic vulnerability of the column, not only in what concerns the collapse risk, but also the magnitude of the expected maximum and residual displacements of the drums, is vital information that can help the authorities decide the necessary interventions. This assessment is not straightforward, not only because fully accurate analyses for the near-collapse state are practically impossible due to the sensitivity of the response to small changes in the geometry and the difficulty in modelling accurately the existing imperfections, but also because the results depend highly on the ground motions characteristics.

In this paper, a risk assessment is performed for the case study of a column of the Parthenon Pronaos in Athens, Greece. To this end, we present a vulnerability assessment approach that accounts for the record-to-record variability. Advanced modelling and numerical analysis tools are combined with performance-based earthquake engineering concepts. The performance-based concept is expanded to classical monuments adopting appropriate performance levels and demand parameters to develop a decision-support system that will take into consideration engineering parameters helping the authorities on deciding upon the interventions required.

2 NUMERICAL MODELLING OF MULTIDRUM COLUMNS

The underlying mathematical problem is strongly non-linear and consequently the modelling of the dynamic behaviour of multidrum columns is quite complex. Even in the case of systems with a single-degree-of-freedom in the two dimensional space, i.e. a monolithic rocking block, the analytical and the numerical analysis is not trivial (Housner [13]) and differs from the approaches followed in modern structural analysis. The dynamic response becomes even more complex in three dimensions, where realistic models have to account for several non-linearities related to the three dimensional motion of each drum and the energy dissipation at the joints. For a more extensive discussion on the dynamic behaviour of such spinal systems we refer to Psycharis [3], Mouzakis *et al.* [8], Dasiou *et al.* [10], Stefanou *et al*. [14] among others.

Herein, we used the Discrete (or Distinct) Element Method (DEM) for the numerical modelling of the seismic response of multidrum systems. DEM may not be the only choice for the discrete system at hand, but it forms an efficient and validated manner for the study of the dynamic behaviour of masonry columns in classical monuments. The Molecular Dynamics (smooth-contact) approach was followed here [15] and the three dimensional DEM code 3DEC [16] was used. This software code provides the means to apply the conceptual model of a masonry structure as a system of blocks which may be considered either rigid, or deformable. In the present study only rigid blocks were used, as this was found to be a sufficient approximation and capable to reduce substantially the computing time. The system deformation is concentrated at the joints (soft-contacts), where frictional sliding and/or complete separation may take place (dislocations and/or disclinations between blocks). As discussed in more detail by Papantonopoulos *et al.* [7], the discrete element method employs an explicit algorithm for the solution of the equations of motion, taking into account large displacements and rotations. The efficiency of the method and particularly of 3DEC to capture the seismic response of classical structures has been already examined by juxtaposing the numerical results with experimental data (Papantonopoulos, *et al*. [7]; Dasiou, *et al*. [11]).

The geometry of the column considered in the present study was inspired by the columns of the Parthenon Pronaos on the Acropolis Hill in Athens. The column has a total height of 10.08 m, being composed of a shaft of 9.38 m and a capital. The real column has 20 flutes; however, the shaft in the numerical model was represented in an approximate manner by a pyramidal segment made of blocks of polygonal 10-sided cross section with diameters ranging from 1.65 m at the base to 1.28 m at the top. The shaft was divided into 12 drums of different height according to actual measurements of the columns of the Pronaos (Figure 1).

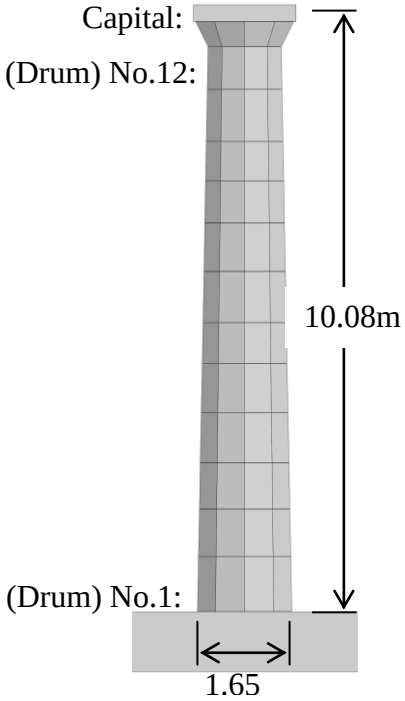

Figure 1. The multidrum column considered in the analyses.

A quite important factor for the numerical analysis is the selection of the appropriate constitutive laws that govern the mechanical behaviour of the joints. In the present paper we made use of a Coulomb-type failure criterion. Moreover, the friction angle was considered equal to 37^o, the cohesion and the ultimate tensile strength were considered equal to zero and

the normal and the shear stiffness of the joints were both considered equal to 1 GPa/m. Note that the stiffness choice might affect considerably the results of the analysis. Furthermore, no connections were considered between the drums, as the only connectors present in the original structure are wooden dowels, the so-called 'empolia', which were used to centre the drums during the erection of the column and not to provide a shear resistant mechanism. The shear strength of the wooden dowels is small and has only marginal effect to the response of the column (Konstantinidis and Makris [6]); for this reason, the wooden dowels were not considered in the numerical model.

3 FRAGILITY ASSESSMENT

Fragility (or vulnerability) curves are a valuable tool for the seismic risk assessment of a system. The seismic fragility F_R is defined as the limit-state probability conditioned on seismic intensity. The seismic intensity can be expressed in terms of magnitude M_w and distance R, resulting to a surface $F_R(M_w,R)$. Therefore, the fragility of a system is the probability that an engineering demand parameter (*EDP*) exceeds a threshold value *edp* and is defined as:

$$F_R(M_w,R)=P(EDP\geq edp\,|M_w,R) \tag{1}$$

Eq. (1) provides a single-point of a limit-state fragility surface, while engineering demand parameters (*EDP*s) are quantities that characterize the system response, e.g., permanent or maximum deformation, drum dislocation. To calculate F_R we performed Monte Carlo Simulation (MCS) using Latin Hypercube Sampling (LHS) for a range of magnitude and distance (M_w, R) scenarios. For this purpose, a large number of nonlinear response history analyses for every M_w–R pair is needed, especially when small probabilities are sought. Therefore, suites of records that correspond to the same M_w and R value must be compiled. Since it is very difficult to come up with such suites of natural ground motion records, we produced synthetic ground motions following the procedure discussed in the following section.

Assuming that seismic data are lognormally distributed, $F_R(M_w,R)$ can be calculated analytically once the mean and the standard deviation of the logs of the *EDP* are calculated, which are denoted as $\mu_{\ln EDP}$ and $\beta_{\ln EDP}$, respectively. Once they are known they can be used to calculate F_R using the normal distribution:

$$F_R=P(EDP\geq edp\,|M_w,R)=1-\Phi\left(\frac{\ln(edp)-\mu_{\ln EDP}}{\beta_{\ln EDP}}\right) \tag{2}$$

where *edp* is the *EDP*'s threshold value that denotes that the limit-state examined is violated and Φ denotes the standard normal distribution.

As the ground motion intensity increases, some records may result in collapse of the structure. When collapsed simulations exist, Eq. (2) is not accurate, since the *EDP* takes an infinite or a very large value that cannot be used to calculate $\mu_{\ln EDP}$ and $\beta_{\ln EDP}$. To handle such cases, Eq. (2) is modified by separating the data to collapsed and non-collapsed ones. The conditional probability of collapse is calculated as:

$$P(C|M_w,R)=\frac{\text{number of simulations collapsed}}{\text{total number of simulations}} \tag{3}$$

If $\mu_{\ln EDP}$ and $\beta_{\ln EDP}$ are the mean and the dispersion of the non-collapsed data respectively, Eq. (2) is modified as follows:

$$P\left(EDP \geq edp \left| M_{\mathrm{w}}, R\right.\right) = P\left(C \left| M_{\mathrm{w}}, R\right.\right) + \left(1 - P\left(C \left| M_{\mathrm{w}}, R\right.\right)\right) \cdot \left(1 - \Phi\left(\frac{\ln\left(edp\right) - \mu_{\ln EDP}}{\beta_{\ln EDP}}\right)\right) \quad (4)$$

4 GENERATION OF SYNTHETIC, HAZARD–CONSISTENT GROUND MOTIONS

The assessment of the seismic reliability of the column of Parthenon that is presented herein is based on synthetic ground motions, representative of near-field sites. The synthetic records were generated using the process that has been proposed by Mavroeidis and Papageorgiou [17], which allows for the combination of independent models that describe the low-frequency (long period) component of the directivity pulse, with models that describe the high-frequency component of an acceleration time history. In the present paper, the generation of the high-frequency component was based on the stochastic (or engineering) approach discussed in detail in Boore [18]. Based on a given magnitude-distance scenario (M_{w}–R) and depending on a number of site characteristics, the stochastic approach produces synthetic ground motions.

It must be noted that, due to the high nonlinear nature of the rocking/wobbling response and the existence of a minimum value of the peak ground acceleration that is required for the initiation of rocking, the high frequency part of the records is necessary for the correct simulation of surrogate ground motions. Long-period directivity pulses alone, although they generally produce devastating effects to classical monuments (Psycharis, *et al*. [5]), might not be capable to produce intense shaking and collapse, as the maximum acceleration of pulses of long period is usually small and not strong enough to even initiate rocking.

Classical monuments were usually constructed on the Acropolis of ancient cities, i.e. on top of cliffs; thus, most of them are founded on stiff soil or rock, and only few of them on soft soil. For this reason, the effect of the soil on the characteristics of the exciting ground motion was not considered in the present analysis. It is noted, though, that, although the directivity pulse contained in near-fault records is not generally affected by the soil conditions, soft soil can significantly alter the frequency content of the ground motion and, consequently, affect the response of classical columns. This effect, however, is beyond the scope of this paper.

4.1 Low frequency pulse

For the long-period component of the synthetic ground motions we applied the pulse model of Mavroeidis and Papageorgiou [17]. This wavelet has been calibrated using actual near-field ground motions from all-over the world. The velocity pulse is given by the expression:

$$V\left(t\right) = 0.5A_{\mathrm{p}}\left[1 + \cos\left(\frac{2\pi f_{\mathrm{p}}}{\gamma_{\mathrm{p}}}\left(t - t_0\right)\right)\right]\cos\left[2\pi f_{\mathrm{p}}\left(t - t_0\right) + \nu_{\mathrm{p}}\right],\ t \in \left[t_0 - \frac{\gamma_{\mathrm{p}}}{2f_{\mathrm{p}}}, t_0 + \frac{\gamma_{\mathrm{p}}}{2f_{\mathrm{p}}}\right] \quad (5)$$

where A_{p}, f_{p}, ν_{p}, γ_{p} and t_0 describe the amplitude of the envelope of the pulse, the prevailing frequency, the phase angle, the oscillatory character (i.e., number of half cycles) and the time shift to specify the epoch of the envelope's peak, respectively. All parameters of Eq. (5) have a clear and unambiguous meaning. For every magnitude – distance scenario (M_{w}–R), the velocity amplitude of the directivity pulse (V_{p}) and the frequency f_{p} were obtained using the expressions produced by Rupakhety *et al.* [19]. Specifically, the mean value of V_{p} was obtained by:

$$\log(V_p) = -5.17 + 1.98 \cdot M_w - 0.14 \cdot M_w^2 - 0.10 \cdot \log\left(R^2 + 0.562\right) \quad (6)$$

where M_w cannot exceed M_{sat}, which is considered equal to 7.0. Thus, for magnitude values above M_{sat}, we set $M_w = M_{sat}$ to obtain V_p using Eq. (6). Similarly, the mean pulse frequency f_p is:

$$\log(1/f_p) = -2.87 + 0.47 \cdot M_w \quad (7)$$

Note that equations (6) and (7) use base 10 logarithms. Also, V_p is not in general equal to the envelope amplitude A_p, but one can be calculated from the other if the phase angle ν_p is known.

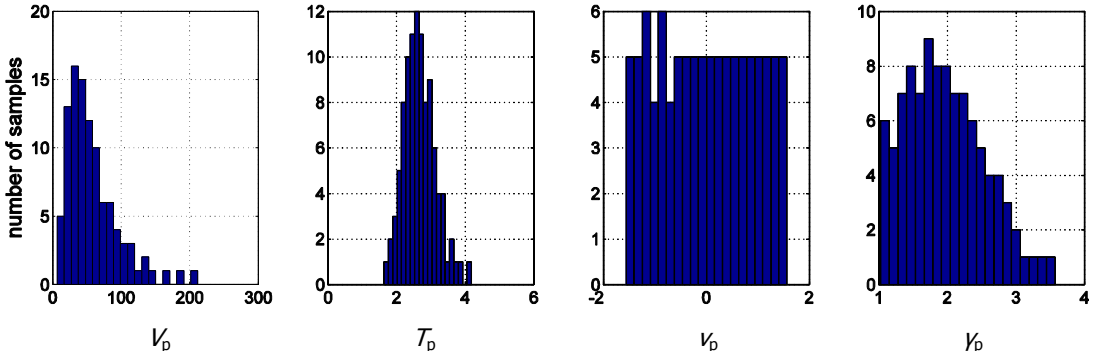

Figure 2. Histogram of the random parameters that describe the low-frequency plot (M_w = 7 and R = 5 km).

We randomly constructed low-frequency pulse-like ground motions using Eq.(5) and giving random values to V_p, f_p, ν_p and γ_p. Sets of pulse-like ground motions were obtained for every M_w–R combination using Latin Hypercube Sampling. We assumed that the logarithms of V_p and f_p follow the normal distribution with standard deviation equal to 0.16 and 0.18, respectively (Rupakhety, *et al*. [19]). The phase angle ν_p was randomly chosen in the $[-\pi/2, \pi/2]$ range. Moreover, being consistent with the data of Mavroeidis & Papageorgiou [17], the number of half cycles γ_p was assumed to follow a normal distribution with mean and standard deviation equal to 1.8 and 0.4, respectively. The distribution of γ_p was left-truncated to one, while V_p and f_p were also left-truncated to zero, ensuring that no negative values were sampled. Figure 2 shows the histogram of the four random parameters used for creating pulses for the M_w = 7 and R = 5 km case.

4.2 High frequency component and combined synthetic strong ground motions

The stochastic approach was selected for modelling the high-frequency component of the ground motions. The stochastic method is discussed in detail in Boore [18] and is based on the ground motion radiation spectrum $Y(M_w,R,f)$, which is the product of quantities that consider the effect of source, path, site and instrument (or type) of motion. By separating the spectrum to its contributing components, the models based on the stochastic method can be easily modified to account for different problem characteristics. The shape and the duration of the ground motions depend on an envelope function $w(M_w,R,t)$. All simulations have been performed using the SMSIM program, freely available from http://www.daveboore.com.

The procedure we used to combine the low and high frequency components is discussed in Mavroeidis and Papageorgiou [17]. Using this approach synthetic ground motion records were constructed for magnitudes M_w in the range 5.5 to 7.5 with a step of 0.5 (five values of

M_w) and distances from the fault R in the range 5 to 20 km with a step of 2.5 km (seven values of R). In total, 35 pairs of M_w–R were considered. For each M_w–R scenario, 100 Monte Carlo Simulations (MCS) were performed for a random sample of V_p, f_p, ν_p, γ_p using Latin Hypercube Sampling to produce the low-frequency pulse, while the high-frequency component was produced using the stochastic method, producing thus 100 random ground motions compatible with the M_w–R scenario considered.

5 PERFORMANCE-BASED RELIABILITY ASSESSMENT OF CLASSICAL MONUMENTS

In order to assess the risk of a monument, the performance levels of interest and the corresponding levels of capacity of the monument need first to be decided. Demand and capacity should be measured with appropriate parameters (e.g. stresses, strains, displacements) at critical locations, in accordance with the different damage (or failure) modes of the structure. Subsequently, this information has to be translated into one or a combination of engineering demand parameters (*EDP*s), e.g., permanent or maximum column deformation, drum dislocation, foundation rotation or maximum axial and shear stresses. For the *EDP*s chosen, appropriate threshold values that define the various performance objectives e.g. light damage, collapse prevention, etc. need to be established.

In the investigation presented here, two engineering demand parameters (*EDP*s) are introduced for the assessment of the vulnerability of classical columns: (a) the maximum displacement at the capital normalized by the base diameter (lower diameter of drum No. 1, see Fig. 2); and (b) the relative residual dislocation of adjacent drums normalized by the diameter of the corresponding drums at their interface. The first *EDP* is the maximum of the normalized displacement of the capital (top displacement) over the whole time history and is denoted as u_{top}, i.e. $u_{top} = \max[u(\text{top})]/D_{base}$. This is a parameter that provides a measure of how much a column has been deformed during the ground shaking and also shows how close to collapse the column was brought during the earthquake. Note that the top displacement usually corresponds to the maximum displacement among all drums. The second *EDP* is the residual relative drum dislocations at the end of the seismic motion normalized by the drum diameter at the corresponding joints and is denoted as u_d, i.e. $u_d = \max(\text{res}u_i)/D_i$. This parameter provides a measure of how much the geometry of the column has been altered after the earthquake increasing thus the vulnerability of the column to future events.

The *EDP*s proposed have a clear physical meaning and allow to easily identify various damage states and setting empirical performance objectives. For example a u_{top} value equal to 0.3 indicates that the maximum displacement was 1/3 of the bottom drum diameter and thus there was no danger of collapse, while values of u_{top} larger than unity imply intense shaking and large deformations of the column, which, however, do not necessarily lead to collapse. It is not easy to assign a specific value of u_{top} that corresponds to collapse, as collapse depends on the 'mode' of deformation, which in turn depends on the ground motion characteristics. For example, for a cylindrical column that responds as a monolithic block with a pivot point at the corner of its base (Figure 3a), collapse is probable to occur for $u_{top} > 1$, as the weight of the column turns to an overturning force from a restoring one when u_{top} becomes larger than unity. But, if the same column responds as a multidrum one with rocking at all joints (Figure 3b), a larger value of u_{top} can be attained without threatening the overall stability. In fact, the top displacement can be larger than the base diameter without collapse, as long as the weight of each part of the column above an opening joint gives a restoring moment about the pole of rotation of the specific part (cf. also video No.1). In the numerical analyses presented here, the maximum value of u_{top} that was attained without collapse was about 1.15.

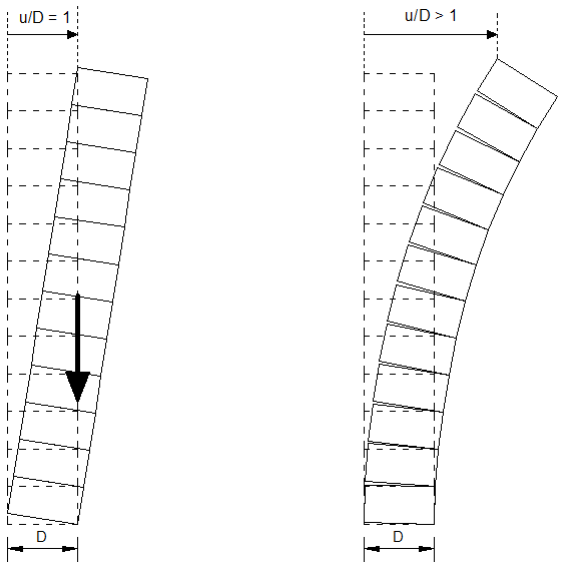

(a) (b)

Figure 3. Top displacement for two extreme modes of rocking: (a) as a monolithic block; (b) with opening of all joints (displacements are shown exaggerated).

u_{top}	Performance level	Description
0.15	Damage limitation	No danger for the column. No permanent drum dislocations expected.
0.35	Significant damage	Large opening of the joints with probable damage due to impacts and considerable residual dislocation of the drums. No serious danger of collapse.
1.00	Near collapse	Very large opening of the joints, close to partial or total collapse.

Table 1. Proposed performance criteria concerning the risk of collapse.

u_d	Performance level	Description
0.005	Limited deformation	Insignificant residual drum dislocations without serious effect to future earthquakes.
0.01	Light deformation	Small drum dislocations with probable unfavourable effect to future earthquakes.
0.02	Significant deformation	Large residual drum dislocations that increase significantly the danger of collapse during future earthquakes.

Table 2. Proposed performance criteria concerning permanent deformation (residual drum dislocations).

Based on the above defined *EDP*s, the performance criteria of Tables 1 and 2 have been adopted. For u_{top}, three performance levels were selected (Table 1), similarly to the ones that are typically assigned to modern structures. The first level (*damage limitation*) corresponds to weak shaking of the column with very small or no rocking. At this level of shaking, no damage nor severe residual deformations are expected. The second level (*significant damage*)

corresponds to intense shaking with significant rocking and evident residual deformation of the column after the earthquake; however, the column is not brought close to collapse. The third performance level (*near collapse*) corresponds to very intense shaking with significant rocking and probably sliding of the drums. The column does not collapse at this level, as $u_{top} < 1$, but it is brought close to collapse. In most cases, collapse occurred when this performance level was exceeded. The values of u_{top} that are assigned at every performance level are based on the average assumed risk of collapse.

Three performance levels were also assigned to the normalised residual drum dislocation, u_d (Table 2). This *EDP* is not directly related to how close to collapse the column was brought during the earthquake, since residual displacements are caused by wobbling and sliding and are not, practically, affected by the amplitude of the rocking. However, their importance to the response of the column to future earthquakes is significant, as previous damage/dislocation has generally an unfavourable effect to the seismic response to future events [20]. The values proposed are based on engineering judgment taking into consideration the size of drum dislocations that have been observed in monuments and also the experience of the authors from previous numerical analyses and experimental tests.

6 FRAGILITY CURVES

The proposed fragility assessment methodology was applied to the classical column of Figure 1. The response of the column was calculated for 35 M_w–R scenarios. For every M_w–R scenario 100 Monte Carlo Simulations (MCS) were performed, thus resulting to 3500 simulations in total.

Figure 4a shows the mean u_{top} displacements of the column and Figure 4b the corresponding u_d displacements. The surface plots of Figure 4a and 4b refer to non-collapsed simulations, while the collapse probabilities as function of magnitude and distance are shown in Figure 4c. Collapse is considered independently of whether it is local (collapse of a few top drums) or total (collapse of the whole column). As expected, the number of collapses is larger for smaller fault distances and larger magnitudes. For example, for $M_w = 7.5$ and $R = 5$ km 40% of the simulations caused collapse, while practically zero collapses occurred for magnitudes less than 6.5.

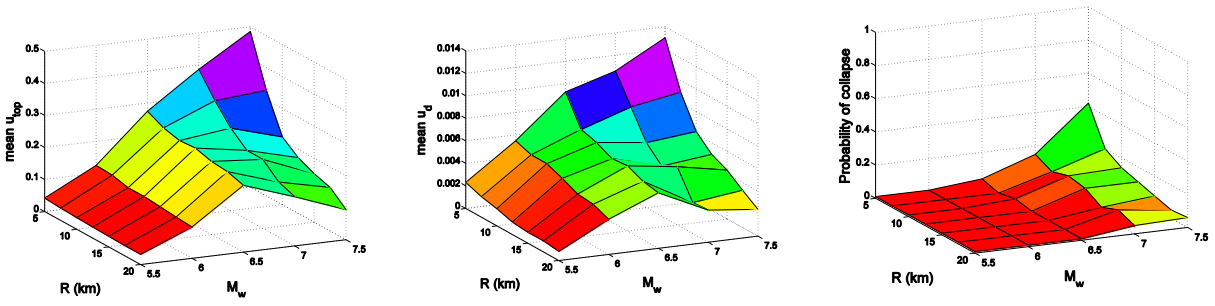

(a) (b) (c)

Figure 4. Mean values of the adopted *EDP*s for the classical column considered: (a) maximum normalised top displacements, u_{top}; (b) normalised residual deformations, u_d; and (c) Collapse probabilities for the multidrum column considered.

An unexpected behaviour is depicted in Figure 4. Concerning the mean top displacement during the seismic motion, Figure 4a shows that for small distances from the fault, up to approximately 7.5 km, the mean value of u_{top} increases monotonically with the magnitude as expected. However, for larger fault distances, the maximum u_{top} occurs for magnitude M_w =

6.5, while for larger magnitudes the top displacement decreases. For example, for R = 20 km, the mean value of u_{top} is approximately 0.4 for M_w = 6.5, while the corresponding value for M_w = 7.5 is about 0.2, i.e. it is reduced to one half. This counter-intuitive response is attributed to the saturation of the *PGV* for earthquakes with magnitude larger than M_{sat} = 7.0 (Rupakhety *et al.* [18], see Eq. (6)) while the period of the pulse is increasing exponentially with the magnitude. As a result, the directivity pulse has small acceleration amplitude for large magnitudes, which is not capable to produce intense rocking (Fig 5).

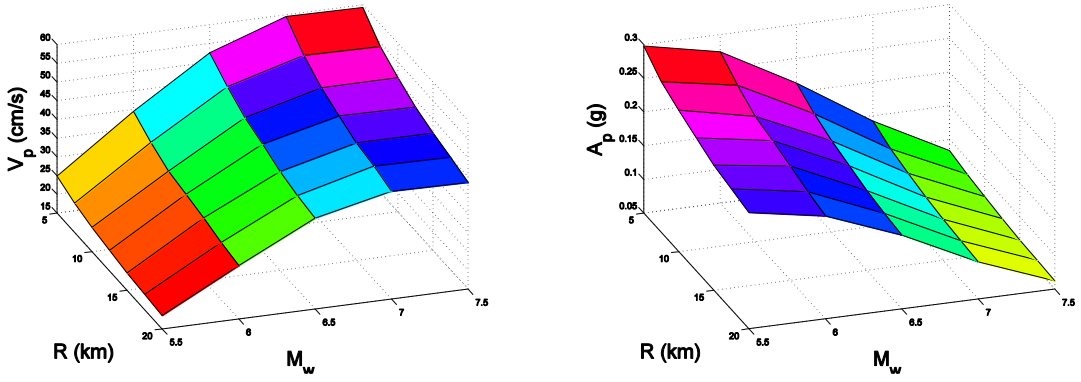

(a) (b)

Figure 5. Variation of the mean value of: (a) the velocity amplitude, and (b) the acceleration amplitude of the directivity pulse, according to Eqs (6) and (7), with the magnitude, M_w, and the distance, R, respectively.

Similar, and probably more pronounced, is the behaviour concerning the permanent drum dislocations u_d shown in Figure 4b. Again, u_d increases monotonically with the magnitude for small values of R only, less than 10 km. For larger distances, u_d increases with M_w up to magnitudes equal to 6.5, when it attains its maximum value. For larger magnitudes smaller permanent deformation of the column occurs.

This 'strange' observation was verified for for both horizontal components of 30 real ground motions from the NGA PEER database [21], recorded in distances ranging from 17 to 23 km: the maximum u_{top} demand occurred for M_w = 6.5, while for higher magnitudes the demand gradually decreased as in the case of the synthetic records. It is interesting to note that most values of u_{top} for natural earthquakes lie below the corresponding line of the synthetic ground motions (Fig. 4a). This was expected, since the synthetic records were constructed considering the directivity pulse with its maximum amplitude, i.e. typically that of the fault-normal direction; however natural ground motions were, in general, recorded in various directions with respect to the fault, and thus contain directivity pulses of reduced amplitude.

Figure 6 shows the fragility surfaces of the classical column for the three performance levels of Table 1 ranging from damage limitation (u_{top} > 0.15) to significant damage (u_{top} > 1). It is reminded that u_{top} > 0.15 means that the maximum top displacement during the ground shaking is larger than 15% of the base diameter and u_{top} > 1 corresponds to intense rocking, close to collapse or actual collapse. When damage limitation is examined, the exceedance probability is of the order of 0.2 for M_w = 6 and increases rapidly for ground shakings of larger magnitude. For the worst scenario among those examined (M_w = 7.5, R = 5 km), the probability that the top displacement is larger than 15% of D_{base} is equal to unity, while in the range M_w = 6.5–7.5 and R > 15 km a decrease in the exceedance probability is observed as discussed above. Similar observations hold for the exceedance of the significant damage limit state (u_{top} > 0.35), but the probability values are smaller. For the near collapse limit state

(u_{top} > 1.0), the probability of exceedance reduces significantly for large distances, even for large magnitudes. It is interesting to note that the u_{top} > 1.0 surface practically coincides with the probability of collapse of Figure 4c, which shows that, if the top displacement reaches a value equal to the base diameter, there is a big possibility that the column will collapse a little later.

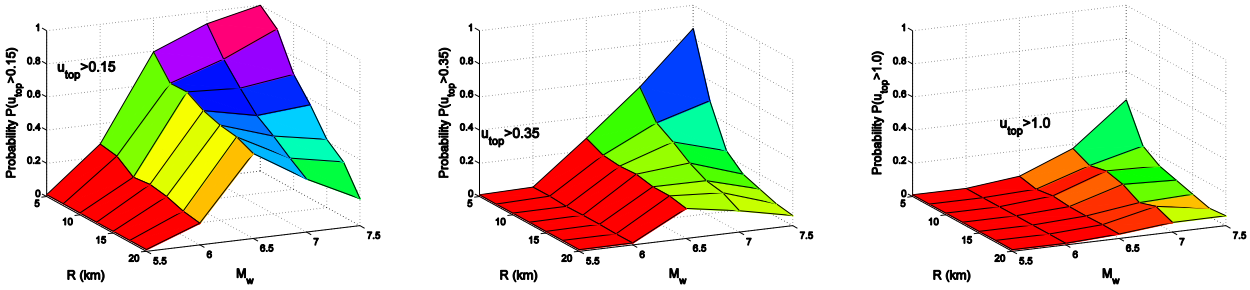

(a) (b) (c)

Figure 6. Fragility surfaces with respect to the maximum capital displacement u_{top} for the performance levels of Table 1: (a) u_{top} > 0.15; (b) u_{top} > 0.35; (c) u_{top} > 1.0.

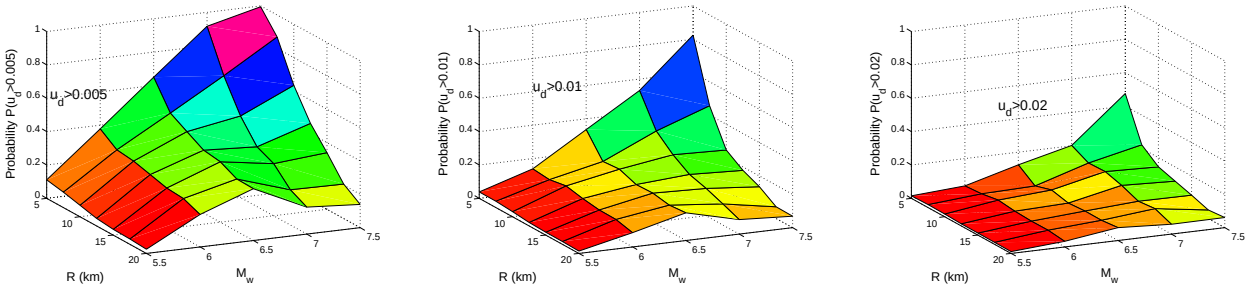

(a) (b) (c)

Figure 7. Fragility surfaces with respect to the permanent drum dislocations, u_d for the performance levels of Table 2: (a) u_d > 0.005; (b) u_d > 0.01; (c) u_d > 0.02.

Figure 7 shows the fragility surfaces when the *EDP* is the normalized permanent drum dislocation, u_d, and considering the performance levels of Table 2. For the limited deformation limit state (u_d > 0.005), probabilities around 0.3 are observed for magnitudes close to 6. Note that, for the column of the Parthenon with an average drum diameter about 1600 mm (Figure 1), u_d > 0.005 refers to residual displacements at the joints exceeding 8 mm. The probability of exceedance of the light deformation performance criterion (u_d > 0.01), which corresponds to residual drum dislocations larger than 16 mm, is less than 0.2 for all earthquake magnitudes examined and for distances from the fault larger than 10 km. The significant deformation limit state (u_d > 0.02) was exceeded only in a few cases.

In Figs 8 and 9 the *PGA* and *PGV* are plotted versus the *EDP*s considered, u_{top} and u_d. The scatter in the results is significant in both cases, slightly smaller for *PGV*. However, clear trends can be identified in the response, especially from Figure 9, showing, in average, a generally linear relation between the deformation (maximum and residual) with *PGV*.

Another conclusion is that very strong earthquakes, with *PGV* that exceeds 150 cm/sec, are required for bringing the column of the Parthenon close to collapse (u_{top} > 1). However, significant dislocations of the drums (u_d > 0.02) can occur for weaker earthquakes with

PGV > 40 cm/sec. These observations are in accordance with findings of previous studies (Psycharis *et al*. [9]).

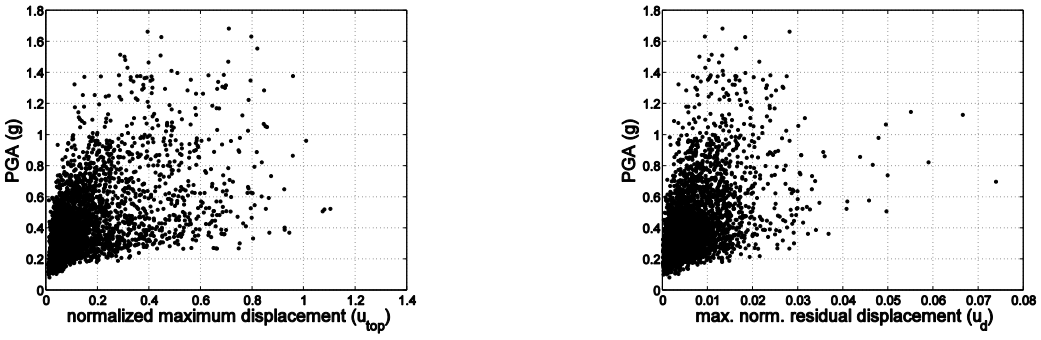

(a) (b)

Figure 8. Scatter plots of *PGA* versus: (a) maximum normalized displacement u_{top}; (b) maximum normalized displacement u_d.

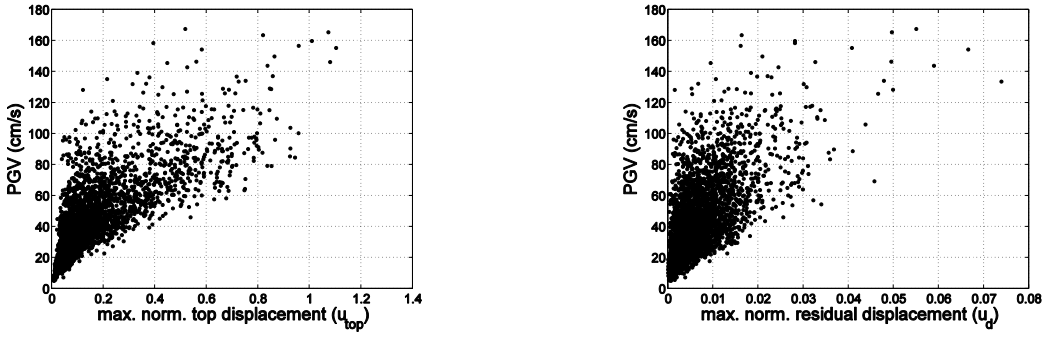

(a) (b)

Figure 9. Scatter plots of *PGV* versus: (a) maximum normalized displacement u_{top}; (b) maximum normalized displacement u_d.

7 CONCLUSIONS

A seismic risk assessment of a column of the Parthenon Pronaos is performed using Monte Carlo simulation with synthetic ground motions which contain a high- and a low- frequency component. The ground motions considered combine the stochastic method and a simple analytical pulse model to simulate the directivity pulse contained in near source records. The fragility analysis demonstrated some of the salient features of these spinal systems under near-fault earthquake excitations which were not realized up to now.

8 ACKNOWLEDGEMENTS

Partial financial support for this study has been provided by the EU research project "DARE" ("Soil-Foundation-Structure Systems Beyond Conventional Seismic Failure Thresholds: Application to New or Existing Structures and Monuments"), which is funded through the 7th Framework Programme "Ideas", Support for Frontier Research – Advanced Grant, under contract number ERC-2—9-AdG 228254-DARE to professor G. Gazetas.

REFERENCES

[1] Allen RH, Oppenheim IJ, Parker AP, Bielak J. On the dynamic response of rigid body assemblies. *Earthquake Engineering and Structural Dynamics*, **14**, 861–876, 1986.

[2] Sinopoli A. Dynamic analysis of a stone column excited by a sine wave ground motion. *Applied Mechanics Reviews* Part 2, **44**, 246–255, 1989.

[3] Psycharis IN. Dynamic behaviour of rocking two-block assemblies. *Earthquake Engineering and Structural Dynamics*, **19**, 555–575, 1990.

[4] Winkler T, Meguro K, Yamazaki F. Response of rigid body assemblies to dynamic excitation. *Earthquake Engineering and Structural Dynamics*, **24**, 1389–1408, 1995.

[5] Psycharis IN, Papastamatiou DY, Alexandris AP. Parametric investigation of the stability of classical columns under harmonic and earthquake excitations. *Earthquake Engineering and Structural Dynamics*, **29**, 1093–1109, 2000.

[6] Konstantinidis D, Makris N. Seismic response analysis of multidrum classical columns, *Earthquake Engineering and Structural Dynamics*, **34**, 1243–1270, 2005.

[7] Papantonopoulos C, Psycharis IN, Papastamatiou DY, Lemos JV, Mouzakis H. Numerical prediction of the earthquake response of classical columns using the distinct element method, *Earthquake Engineering and Structures Dynamics*, **31**, 1699–1717, 2002

[8] Mouzakis H, Psycharis IN, Papastamatiou DY, Carydis PG, Papantonopoulos C, Zambas C. Experimental investigation of the earthquake response of a model of a marble classical column, *Earthquake Engineering and Structures Dynamics*, **31**, 1681–1698, 2002.

[9] Psycharis IN, Lemos JV, Papastamatiou DY, Zambas C, Papantonopoulos C. Numerical study of the seismic behaviour of a part of the Parthenon Pronaos, *Earthquake Engineering and Structural Dynamics*, **32**, 2063–2084, 2003.

[10] Dasiou M-E, Mouzakis HP, Psycharis IN, Papantonopoulos C, Vayas I. Experimental investigation of the seismic response of parts of ancient temples. *Prohitech Conference 2009 Rome*, 21-24 June, 2009.

[11] Dasiou M-E, Psycharis IN, Vayias I. Verification of numerical models used for the analysis of ancient temples. *Prohitech Conference 2009 Rome*, 21-24 June, 2009.

[12] Stefanou I, Psycharis IN, Georgopoulos I-O. Dynamic response of reinforced masonry columns in classical monuments, *Construction and Building Materials*, **25**, 4325–4337, 2011.

[13] Housner GW. The behavior of inverted pendulum structures during earthquakes, *Bulletin of Seismological Society of America*, **53**, 403–417, 1963.

[14] Stefanou I, Vardoulakis I, Mavraganis A. Dynamic motion of a conical frustum over a rough horizontal plane. *International Journal of Non-Linear Mechanics*, **46**, 114-124, 2011.

[15] Cundall PA, Strack OD. A discrete numerical model for granular assemblies, *Geotechnique*, **29**, 47–65, 1979.

[16] Itasca Cosulting Group, Inc., 3-dimensional Distinct Element Code (3DEC), *Theory and Background*, Minneapolis, Minnesota, 1998

[17] Mavroeidis GP, Papageorgiou AS. A mathematical representation of near-fault ground motions. Bulletin of Seismological Society of America, **93**, 1099–1131, 2003.

[18] Boore DM. Simulation of Ground Motion Using the Stochastic Method. *Pure and Applied Geophysics*, **160**, 653–676, 2003

[19] Rupakhety E, Sigurdsson SU, Papageorgiou AS, Sigbjörnsson R. Quantification of ground-motion parameters and response spectra in the near-fault region, *Bulletin of Earthquake Engineering*, **9**, 893–930, 2011.

[20] Psycharis I. A Probe into the Seismic History of Athens, Greece from the Current State of a Classical Monument, *Earthquake Spectra*, **23**, 393–415, 2007.

[21] Pacific Earthquake Engineering Research Center: NGA Database. http://peer.berkeley.edu/nga